JPET Fast Forward. Published on February 22, 2017 as DOI: 10.1124/jpet.117.240382
This article has not been copyedited and formatted. The final version may differ from this version.

Journal of Pharmacology and Experimental Therapeutics

Comprehensive Characterization of Mouse UDP-Glucuronosyltransferase (Ugt) belonging to the Ugt2b Subfamily: Identification of Ugt2b36 as the Predominant Isoform Involved in Morphine Glucuronidation

Ayumi Kurita, Yuu Miyauchi, Shin'ichi Ikushiro, Peter I. Mackenzie, the late Hideyuki Yamada[1], and Yuji Ishii

Laboratory of Molecular Life Sciences, Graduate School of Pharmaceutical Sciences, Kyushu University, Fukuoka, Japan (A.K., Y.M., H.Y., Y.I.)

Department of Biotechnology, Faculty of Engineering, Toyama Prefectural University, 5180 Kurokawa, Imizu, Toyama 939-0398, Japan (S. I.)

Department of Clinical Pharmacology and Flinders Centre for Innovation in Cancer, Flinders University School of Medicine, Flinders Medical Centre, Bedford Park, SA, Australia (P.I.M.)

Running Title: Ugt2b36 as a mouse morphine Ugt

To whom correspondence should be addressed: Yuji Ishii, Laboratory of Molecular Life Sciences, Graduate School of Pharmaceutical Sciences, Kyushu University, 3-1-1 Maidashi, Higashi-ku, Fukuoka 812-8582, Japan, Tel.: +81-92-642-6586; Fax: +81-92-642-6588; E-mail: ishii@phar.kyushu-u.ac.jp

Number of text pages: 39

Number of tables: 3

Number of figures: 6

Number of references: 54

Words in Abstract: 233

Words in Introduction: 716

Words in Discussion: 1441

Supplemental figure: 2

Supplemental table: 3

Abbreviations: CYP and P450, cytochrome P450; MLM, mouse liver microsomes; HRP, horseradish peroxidase; PCR, polymerase chain reaction, Ugt and UGT, UDP-glucuronosyltransferase; UDPGA, UDP-glucuronic acid; M-3-G, morphine-3-glucuronide; M-6-G, morphine-6-glucuronide; E3G, estradiol-3-glucuronide; E17G, estradiol-17-glucuronide; 4-MU, 4-methylumbelliferone; SDS-PAGE, SDS-polyacrylamide gel electrophoresis; EndoH, endoglycosidase H; PVDF, polyvinyldene difluoride

Abstract

UDP-Glucuronosyltransferases (UGTs) are classified into three subfamilies, Ugt1a, 2b, and 2a, in mice. In the *Ugt1a* subfamily, *Ugt1a1* and *1a6* appear to correspond to human *UGT1A1* and *1A6*. The mouse is an important animal used for investigations but the substrate specificities of Ugt isoforms belonging to the 2b subfamily in mice remain largely unknown. To address this issue, we characterized the substrate specificity of all isoforms of the Ugt2b subfamily expressed in mouse liver. The cDNAs of Ugt1a1, Ugt2a3 and all the Ugt2b isoforms expressed in the liver were reverse-transcribed from total RNA of male FVB-mouse liver and amplified. A baculovirus-Sf9 cell system for expressing each Ugt was established. Of all the Ugts examined, Ugt2b34, 2b36, and 2b37 exhibited the ability to glucuronidate morphine with Ugt2b36 the most active in this regard. Ugt1a1, but also Ugt2b34, 2b36, and 2b37 to a lesser extent preferentially catalyzed the glucuronidation of 17β-estradiol on the 3-hydroxyl group (E3G). With these isoforms, E3G formation by Ugt1a1 was efficient. However, Ugt2b5 exhibited a preference for the 17β-hydroxyl group (E17G). Ugt2b1 and Ugt2a3 formed comparable levels of E3G and E17G. Ugt2b1 and 2b5 were the only isoforms involved in chloramphenicol glucuronidation. As Ugt2b36 is highly expressed in the liver, it is most likely that Ugt2b36 is a major morphine Ugt in mouse liver. Regarding E3G formation, Ugt1a1, like the human homologue, seems to play an important role in the liver.

Introduction

Following administration, drugs are absorbed, distributed, metabolized and then eliminated. Usually, a fraction of the drugs administered are eliminated in unchanged form. However, in many cases, drugs are metabolized to increase their hydrophilic properties prior to elimination. Drug metabolism reactions are categorized into phase I and II reactions. Oxidation, reduction and hydrolysis are categorized as a phase I reactions. On the other hand, conjugations are categorized as Phase II reactions. In phase I reactions, P450 cytochromes (P450, CYPs) play a key role (Guengerich, 2006). However, regarding conjugation reactions, glucuronidation contributes to approximately 35% of phase II reactions (Evans and Relling, 1999). UDP-Glucuronosyltransferases (UGTs, Ugts) catalyze glucuronidation and the classical view that P450-catalyzed hydroxylations precede glucuronidation of the metabolites formed by P450 holds true for many drugs. However, compounds such as morphine are cleared primarily by direct glucuronidation without requiring P450 enzymes (Yoshimura et al., 1969). Further, UGTs occupy 2nd place after P450 in terms of drug clearance (Williams, et al., 2004). Thus, it is important to investigate UGT-catalyzed reactions.

The use of morphine to treat pain associated with cancer is widely recommended (World Health Organization, 1996). However, there is also an accompanying issue of morphine overdosing and considerable numbers of patients medicated with morphine die (Okie, 2010). It is glucuronidated in vivo to form a main metabolite, morphine-3-glucuronide (M-3-G), and a minor metabolite, morphine-6-glucuronide (M-6-G) (Yoshimura et al., 1969). Although M-3-G is a non-analgesic metabolite, M-6-G is a more potent metabolite than the parent morphine (Shimomura et al., 1971). It is known that there are species differences in M-6-G formation. A

relatively large amount of M-6-G is formed in humans and guinea pigs after morphine treatment while only a small amount of M-6-G is formed in rats and mice (Oguri et al., 1970; Svensson et al., 1982; Kuo et al., 1991). In humans, UGT2B7 mainly catalyzes the formation of M-3-G and M-6-G (Coffman et al., 1997; Stone et al., 2003) while, in guinea pigs, UGT2B21 catalyzes M-3-G formation (Ishii et al., 2001). In rats, UGT2B1 catalyzes M-3-G formation (Pritchard et al., 1994). In mice, Ugt2b1 is considered as orthologous to rat UGT2B1 on the basis of sequence similarity (Mackenzie et al., 2005). However, its function has yet to be characterized. Although it is reasonable to suppose that the mouse Ugt involved in morphine glucuronidation probably belongs to the Ugt2b subfamily, mouse Ugt isform(s) involved in morphine glucuronidation are so far unknown. Since the mouse is a very important experimental animal, it is expected that characterization of the Ugt isoform(s) involved in morphine metabolism will help in the extrapolation of pre-clinical trial data to humans.

To date, there are 21 Ugt isoforms known to be expressed in mice which belong to the Ugt1a, 2a, 2b and 3a subfamilies (Mackenzie et al., 2005). These are mainly expressed in the liver and intestine but, in some cases, in brain and lung (Buckley and Klaassen, 2007). The gene structure of the UGT1A subfamily involves a variable exon 1 and common exons 2 to 5 (Iyanagi, 1991; Ritter et al., 1992). The UGT1 locus consists of variable first exons and four shared exons in a tandem array. Since such gene structures are to a degree conserved among mouse, rat and human, at least, Ugt1a1 and 1a6 in mice seem orthologous to UGT1A1 and 1A6 in humans and rats, respectively (Mackenzie et al., 2005). This is supported by a study using Ugt1a locus null-mice (Nguyen et al., 2008). However, for the mouse Ugt2b subfamily, all Ugt2b isoforms except Ugt2b1 have unique numbers since it is difficult to define orthologues. There are many studies

of changes in the expression level of Ugt isoforms in mice involving disease, chemicals or genetically-engineered model animals (Buckley and Klaassen, 2007; 2009a; 2009b; Lu et al., 2010). Further, knocking out the Ugt2b locus in mice has been reported and characterized (Fay et al., 2015). However, characterization of mouse Ugt isoforms, except 1a6 (Uchihashi et al., 2012; 2013), has not been reported and it would be of great interest to understand the function of mouse Ugts, especially the Ugt2b subfamily.

In this study, with reference to a mouse genome database, we have cloned cDNAs encoding all Ugt isoforms belonging to the Ugt2b subfamily and established their expression system. We found that Ugt2b36 is the predominant morphine Ugt in mice.

Materials and Methods

Chemicals

Morphine hydrochloride was purchased from Takeda Pharmaceutical Industry, Co., Ltd. (Osaka, Japan). 4-Methylumbelliferone (4-MU), estradiol 3β-D-glucuronide (E3G), estradiol 17β-D-glucuronide (E17G) and alamethicin were purchased from Sigma-Aldrich (St. Louis, MO). Chloramphenicol, UDP-glucuronic acid (UDPGA) trisodium salt and 4-MU-β-D-glucuronide were obtained from Nakalai Tesque (Kyoto, Japan). 17β-Estradiol was purchased from Wako Pure Chemical Industries, Ltd. (Osaka, Japan). Chloramphenicol glucuronide (Sigma-Aldrich) was a generous gift from Dr. Yoshihisa Kato (Kagawa School of Pharmaceutical Sciences, Tokushima Bunri University, Japan). M-3-G was synthesized by a method described previously (Yoshimura et al., 1968). All other reagents were of the highest grade commercially available.

Animals

Animal experiments in this study were conducted following the approval of the Ethics Committee for Animal Experiments of Kyushu University. Male FVB mice (7 weeks-old) were obtained from CLEA Japan (Tokyo, Japan) and were maintained for one week with free access to water and a suitable diet under a 7 a.m. to 7 p.m. light/dark cycle. For isolation of total RNA, liver tissue was quickly cut into small fragments, immediately immersed in liquid nitrogen, and stored at -80ºC until required. For preparation of microsomes, the liver was removed and perfused with ice-cold saline, and the microsomes were prepared by differential centrifugation as described previously (Oguri et al., 1996). The resulting microsomes were re-suspended in 0.25 M sucrose, frozen in liquid nitrogen, and stored at -80˚C.

RNA Extraction and Reverse Transcription Polymerase Chain Reaction (RT-PCR)

Total RNA was extracted from male mouse-liver tissue using an RNeasy® Mini Kit (QIAGEN, Hilden, Germany) and the RNA was quantified by absorbance at 260nm. cDNA was prepared from 250 μg total RNA in 15 μL of total volume using a Primescript™ RT Reagent Kit (Takara Bio, Shiga, Japan).

Amplification and cloning of cDNAs encoding mouse Ugt isoforms

PCR primers were designed to amplify cDNAs encoding mouse Ugt isoforms based on the genome database. The GeneBank accession numbers of the reference sequences are as follows: Ugt1a1 (AAH93516), Ugt2a3 (AAH25795), Ugt2b1 (AAH27200), Ugt2b5

(AAH28262)(Kimura and Owens, 1987), Ugt2b34 (EDL37970), Ugt2b35 (AAI13790), Ugt2b36 (AAI41233), Ugt2b37 (AAH29487), and Ugt2b38 (AAH69923). The primers used are listed in Table 1, and the PCR conditions are described (Supplemental Tables 1 and 2). The PCR products were extracted from agarose gels and purified using a QIAquick® Gel Extraction Kit (QIAGEN). Purified PCR products with restriction sites at both ends were digested in *Not*I and *Xho*I, then cloned into pFastBac1 restricted with the same enzymes. The sequencing reaction was carried out using a Big Dye® Terminator v3.1 Cycle Sequencing Kit (Life Technologies). Then, cDNA sequences were confirmed by an ABI 3130xl Genetic Analyzer. There were only non-synonymous mutations in Ugt1a1 (T915G) and Ugt2b5 (G693A) on the basis of the reference sequences (Kong et al., 1993; Kimura and Owens, 1987). The sequences of the other Ugt-cDNAs amplified were identical to each reference. Therefore, all the Ugt cDNAs amplified in this study were regarded as wild-type.

Expression of Recombinant Ugts

Bacmid of the recombinant Ugts was prepared from *Escherichia coli* DH10Bac™ strain (Life Technologies)-transformed with recombinant pFastBac1. Recombinant baculovirus was prepared using the Bac-to-Bac® Baculovirus Expression System (Life Technologies) as described previously (Ishii et al., 2014). The amplification of baculovirus was repeated usually two- to three-times to obtain the virus with a titer of over 1.0×10^7 plaque-forming units/ml. NucleoSpin® Blood (Macherey-Nagel, Düren, Germany) was used for purification of the viral DNA and their titers were determined using a BacPAK™ qPCR Kit (Clontech, Mountain View, CA). For expression of recombinant enzymes, Sf9 cells (2.0×10^6 cells/ml, 200 ml) were

infected with recombinant baculovirus with a multiplicity of infection (MOI = 0.01 PFU/cell) in an Erlenmeyer flask (Corning, New York), and harvested 40 h after infection by low speed centrifugation. Microsomes were prepared from the transfected cells as described by Ishii et al. (2014). Preparation of recombinant UGT2B7 baculovirus was described previously (Miyauchi et al., 2015; Jin et al., 1993). The UGT2B7 baculosomes used in this study were prepared similarly to the mouse Ugt2b isoforms as described above.

Immunoblotting

Microsomes separated by SDS-polyacrylamide gel electrophoresis (SDS-PAGE) were electroblotted on a polyvinyldene difluoride (PVDF) membrane (Millipore, Bedford, MA). Each of the Ugts was detected using goat anti-mouse low-p*I* formed UGT antibody (Mackenzie et al., 1984) or rabbit anti-UGT2B antibody (Kasai et al., 2004). As secondary antibodies, horseradish peroxidase (HRP)-rabbit anti-goat IgG (MP Biomedicals, Santa Ana, CA) and HRP-donkey anti-rabbit IgG (GE Healthcare, Little Chalfont, UK) were used. Clarity™ Western ECL Substrate (Bio-Rad, Hercules, CA) was used as the substrate of HRP, and the chemiluminescence emitted was analyzed using a ChemiDoc™ MP System (Bio-Rad, Hercules, CA).

Endoglycosidase H (EndoH)-treatment

Treatment of baculosomes with EndoH was performed as described previously (Nakamura et al., 2016).

Glucuronidation Assay

The glucuronidation of morphine at the 3-hydroxyl group was carried out by a method reported previously (Nurrochmad et al., 2010) with slight modifications. Microsomes were pretreated with alamethicin (50 μg/mg protein) on ice for 30 min. The method used 200 μg protein in a 0.3 ml reaction except for kinetic analysis (100 μg protein). For mouse liver microsomes (MLM), 100 μg protein was used. For the kinetic study, the substrate concentration ranged from 0.1 to 6 mM. Incubation was performed at 37ºC for 120 min but a 90 min incubation was used in the kinetic analysis. M-3-G was detected by high-performance liquid chromatography (HPLC). A D-2000 Elite HPLC system equipped with an automatic sampler (model L-2200), pump (L-2130), column oven (L-2300), and fluorescence detector (L-2485) (Hitachi High Technologies Co., Tokyo, Japan) were used for the chromatographic analysis. Separation was achieved using a Nova-Pak® C18 column (4 μm, 8 × 100 mm, Waters, Milford, MA) housed in a column heater that was set at 25ºC. The mobile phase was a mixture of eluent A (20 mM sodium phosphate, pH 2.2) and eluent B (eluent A : acetonitrile = 80 : 20) at a ratio of 90 : 10 and this condition was maintained for 35 min. The flow rate was set at 0.8 ml/min. M-3-G was quantified by fluorescence detection (excitation wavelength 210 nm and emission wavelength 350 nm). Under these conditions, the retention time of M-3-G was 13.6 min.

The 4-MU glucuronidation activity and glucuronidation of 17β-estradiol at the 3- and 17-hydroxyl groups were determined by the method described previously (Nishimura et al., 2007) with slight modifications. Unless otherwise stated, the incubation mixture consisted of 50 mM potassium phosphate buffer (pH 7.4), 5 mM $MgCl_2$, 2 mM UDPGA, 100 μg each recombinant Ugt baculosomes, and 200 μM 4-MU or 17β-estradiol (1 mM or 10 μM). Substrates

were dissolved in methanol, and the final concentration of methanol in the incubation mixture was 0.5%. Incubation was performed at 37ºC for 1 hr and the glucuronides were detected by HPLC. The eluted solution of 4-MU was prepared by mixing eluent A (20 mM sodium phosphate, pH 2.2) and eluent B (acetonitrile): the concentration of acetonitrile was 20% for 9.9 min, then increased to 50% for 0.1 min, held at 50% for 3 min and, finally, reduced to 20% and held there for 7 min. The flow rate was set at 0.8 ml/min. 4-MU-glucuronide was quantified by fluorescence detection (excitation 315 nm and emission 375 nm). Under these conditions, the retention time of 4-MU-glucuronide was 5.1 min. For detection of 17β-estradiol-3-glucuronide (E3G) and 17-glucuronide (E17G), a solution mixing eluent A (20 mM sodium phosphate, pH 2.2) and eluent B (acetonitrile) was prepared: the concentration of acetonitrile was 35% for 19.9 min, then increased to 60% for 0.1 min, held at 60% for 5 min and, finally, reduced to 35% and held there for 5 min. Then, the column was equilibrated with the initial condition before analysis of new sample. The flow rate was set at 1 ml/min. E3G and E17G were quantified by fluorescence detection (excitation 210 nm and emission 300 nm). Under these conditions, the retention times of E3G and E17G were 3.9 and 4.6 min, respectively. In kinetic assays for estradiol, the substrate concentration was varied ranging from 1 to 100 μM. For MLM and Ugt1a1-expressing microsomes, 100 μg protein was used. Incubation was performed at 37˚C for 1h.

Glucuronidation of chloramphenicol was assayed according to Kato et al. (2000) with slight modifications. Unless otherwise stated, the incubation mixture consisted of 50 mM Tris-HCl buffer (pH 7.4), 5 mM $MgCl_2$, 2 mM UDPGA, each recombinant Ugt baculosome (300 μg protein), and 5 mM chloramphenicol. Microsomes were pretreated with alamethicin as described

above. Chloramphenicol was dissolved in methanol, and the final concentration of methanol in the incubation mixture was 0.5%. Incubation was performed at 37ºC for 2 hr. The chloramphenicol glucuronide produced was quantified by HPLC coupled to a UV detector (model L-2400) (Hitachi High Technologies) at 278 nm. The eluted solution of chloramphenicol was prepared by mixing eluent A (20 mM sodium phosphate, pH 2.2) and eluent B (acetonitrile): the concentration of acetonitrile was 20% for 9.9 min, then increased to 50% for 0.1 min, held at 50% for 7 min and, finally, reduced to 20% and held there for 3 min. The flow rate was set at 0.8 ml/min and the retention time of chloramphenicol glucuronide under these conditions was 11.6 min.

Construction of a phylogenetic tree of mouse Ugts and the UGTs in other species

The amino acid sequences of mouse Ugts examined in this study were compared with those of human UGT amino acids. In addition, rat (*rattu norvegicus*) UGT2B1 (Mackenzie, 1987) and guinea pig (*cavia porcellus*) UGT2B21 (Ishii et al., 2001), which are known to glucuronidate morphine, were used for comparison of the amino acids. The following GenBank accession-numbers were used: human UGT1A1 (AAI28415)(Ritter et al., 1991), human UGT2A3 (AAI30534)(Court et al., 2008), human UGT2B7 (AAH30974)(Ritter et al., 1990), human UGT2B10 (AAI13650)(Jin et al., 1994), human UGT2B17 (EAW55622)(Beaulieu et al., 1996), human UGT2B28 (NP_001064)(Lévesque et al., 2001), rat UGT2B1 (NP_775417), guinea pig UGT2B21 (BAB82476). A distance-based neighbor-joining phylogenetic tree was generated (Saitou and Nei, 1987). The reliability of the phylogeny was tested by bootstrap analysis with 1000 replicates. The bootstrap values are indicated in the neighbor-joining

consensus tree and the phylogenetic tree was constructed by ClustalW (http://clustalw.ddbj.nig.ac.jp/).

Data Analysis

Data analysis for the kinetics was carried out using GraphPad Prism 5.04 software (GraphPad software, La Jolla, CA). Kinetic data were fitted to a Michaelis-Menten model using the equation below:

$$V = Vmax \times S / Km + S$$

where V is the reaction rate, Vmax is the maximum enzyme velocity, S is the substrate concentration, and Km is the substrate concentration giving half Vmax.

In the case of UGT2B7, the kinetic data were fitted to a sigmoidal model defined by the equation below:

$$V = Vmax \times S^n / (S_{50}{}^n + S^n)$$

where S_{50} is the substrate concentration giving half Vmax, and *n* is the Hill coefficient.

Other Method

Protein concentrations were determined by the method of Lowry et al. (1951) with bovine serum albumin as a standard.

Results

The substrate specificities of the Ugt2b subfamily mouse isoforms were studied. cDNAs encoding all the mouse Ugt2b subfamily isoforms were amplified by nested RT-PCR from mouse liver mRNA. Ugt1a1 and 2a3 cDNA were also cloned and expressed by the baculovirus-Sf9 system. Their microsomes were prepared and the expression of these Ugt proteins was confirmed by western blotting using an antibody toward a low-p*I* mouse Ugt (Fig. 1A). Although we carried out the expression of Ugts under the same conditions, the intensity of bands varied, possibly due to differences in immuno-reactivity between isoforms. Thus, we compared the Ugt content in microsomes by use of an anti-peptide antibody which recognizes the same epitope in all the mouse Ugts examined in this study (Fig. 1B). The antibody was originally produced against a common epitope (KWIPQNDLLGHPK; the residues 355-367 of UGT2B7) of human UGT2B isoforms (Supplemental Table 2)(Kasai et al., 2004). The corresponding sequence of Ugt2b1 is completely identical to this epitope but differs to that of Ugt2b5 by a single substitution at residue 358 from Ile (Ugt2b1) to Leu (Ugt2b5). Despite this difference, the band intensities of Ugt2b1 and Ugt2b5 in Fig. 1B are comparable. The Ugt2b5 epitope is shared among the other mouse Ugt2b isoforms and Ugt1a1 except for Ugt2b1 and Ugt2b34. Ugt2b34 shares the sequence of Ugt2b1 but for a single amino-acid difference from

Pro (Ugt2b1) to Ser (Ugt2b34) at residue 369. Further, Ugt2a3 shares the epitope sequence of Ugt2b1 except for a single amino acid substitution at residue 355 from Lys (Ugt2b1) to Asn (Ugt2a3). Hence, it seems reasonable to suppose that the antibody can recognize all mouse Ugt2b subfamily isoforms, Ugt1a1 and Ugt2a3 examined in this study to the same degree. With the exception of Ugt2b35, all mouse Ugt2b forms as well as Ugt1a1 and Ugt2a3 appeared as a single band on SDS-PAGE (Fig. 1A). In case of Ugt2b35, the microsomes were treated with EndoH prior to SDS-PAGE (Fig. 1B). Thus it was possible to normalize the relative Ugt content in the microsomes expressing each mouse Ugt isoform when evaluating their catalytic property.

Using 4-MU as a substrate, all the Ugt isoforms examined exhibited activity. However, substrate preferences differed among isoforms. With 4-MU, very high activity was observed for Ugt2b5, Ugt2b34, 2b36 and Ugt1a1 whereas Ugt2b1 and 2b35 showed intermediate activity and Ugt2b37, 2b38 and 2a3 exhibited much lower activity (Fig. 2). Glucuronidation of steroids is typical of UGT isoforms. We used 17β-estradiol which possesses both an aromatic 3-hydroxyl group and a 17β-hydroxyl group as a substrate. Keeping the substrate concentration at 1 mM, we examined which isoform(s) is mainly involved in the glucuronidation of this steroid. Of the Ugt isoforms examined in this study, Ugt1a1 is the main catalyst for glucuronidation at the 3-hydroxyl group (Fig. 3). Although there were measurable activities for the other isoforms, these were far lower than that of Ugt1a1. In addition, their specificities for the 17β-hydroxyl group were significantly different (Fig. 3). At 1 mM 17β-estradiol, Ugt2b5 exhibited high activity followed by Ugt2b1 which also exhibited considerable activity, while Ugt2b34, 2b35, 2b38 and 2a3 exhibited lower activity. However, the activities of Ugt2b36, 2b37 and 1a1 were below the detection limit. Also, at 10 μM 17β-estradiol, Ugt2b34, 2b35, 2b38 and 2a3 did not

have any substantial activity with regard to the 17-hydroxyl group. Ugt2b5 exhibited high activity followed by Ugt2b1 at a low substrate condition as well.

For glucuronidation of morphine, Ugt2b36 exclusively catalyzed this reaction while Ugt2b34, 2b35 and 2b37 exhibited very low activity (Fig. 4A). Also, no activity was detected for Ugt2b1, 2b5, 2b38, 1a1 and 2a3. Under the assay conditions used, Ugt2b36 only catalyzed glucuronidation at the 3-hydroxyl group of morphine (M-3-G formation) but not at the 6-hydroxyl group (M-6-G formation). Glucuronidation of chloramphenicol was catalyzed only by Ugt2b1 and 2b5 (Fig. 4B), with Ugt2b5 exhibiting the higher activity. The other isoforms examined in this study showed no substantial activity with regard to chloramphenicol.

In the kinetic study, Ugt2b36 microsome-catalyzed morphine glucuronidation was fitted to a Michaelis-Menten equation similar to that of MLM (Fig. 5A, Table 2) while human UGT2B7, the predominant isoform participating in hepatic morphine glucuronidation, exhibited sigmoidal kinetics (Fig. 5C, Table 2). Again, the Vmax of MLM was higher than that of Ugt2b36, but it cannot be simply compared because the Ugt2b36 content was not normalized between MLM and the Ugt2b36-expressing microsomes. However, the Kms of Ugt2b36 and MLM for morphine were comparable. The Km of Ugt2b36 was lower than that of UGT2B7 while the intrinsic clearance of Ugt2b36 was higher than that of UGT2B7. It is reasonable to suppose that Ugt2b36 is a representative isoform involved in morphine glucuronidation in mouse liver. On the basis of the expressed enzymes in this study, mouse Ugt2b36 exhibits higher activity than human UGT2B7. Regarding the kinetics of estradiol 3-glucuronidation activity, Ugt1a1 and MLM were examined (Fig. 6, Table 3). Again, the Vmax of MLM was higher than that of Ugt1a1, but it cannot be simply compared because the Ugt1a1 content was not normalized between MLM and

the Ugt1a1-expressing microsomes. However, the Km of Ugt1a1 for the 3-hydroxyl group of estradiol was smaller than MLM. This suggested that glucuronidation at the 3-hydroxyl group of estradiol was catalyzed by Ugt1a1.

Discussion

There are a number of reports describing changes in the level of mouse Ugt isoforms depending on gender, disease or chemicals (Buckley and Klaassen, 2007; 2009a; 2009b). Although there is a study of the substrate specificity of mouse Ugt1a6a and 1a6b (Uchihashi et al., 2012), the substrate specificity of all mouse Ugts, except Ugt1a6, remained to be clarified. In this study, we comprehensively characterized the substrate specificity of Ugt1a1, Ugt2a3 and all the Ugt2b subfamily isoforms expressed in mouse liver. We demonstrated for the first time that Ugt2b36 is the predominant Ugt isoform involved in morphine glucuronidation in mouse liver. Anti-mouse low-p*I* form UGT antibody (Mackenzie et al., 1984) recognized all the mouse Ugts examined in this study. Of the Ugts examined, Ugt2b36 was strongly recognized by this antibody. Since the purified low-p*I* form mouse Ugt catalyzed morphine glucuronidation (Mackenzie et al., 1984), it is reasonable to suppose that the purified preparation contained Ugt2b36. Although the infection of Sf9 with baculovirus encoding each Ugt isoform was carried out with the same MOI, the intensity of the Ugt bands varied (Fig. 1A). Therefore, we evaluated relative Ugt levels with an anti-UGT2B antibody which recognizes all the mouse Ugt2b subfamily isoforms, Ugt1a1 and Ugt2a3 to a comparable extent (Fig. 1B). This enabled normalization of the Ugt activity on the

basis of relative Ugt protein levels. The level of each recombinant Ugt was within the range of the Ugt level observed in the MLM. Based on relative UGT levels, the glucuronidation of morphine was catalyzed almost exclusively by Ugt2b36. Following Ugt2b36, morphine glucuronidation activity was exhibited by Ugt2b34, 2b35 and 2b37 but this was very low compared to Ugt2b36. Thus, it is reasonable to conclude that Ugt2b36 is the predominant isoform participating in morphine glucuronidation in mouse liver. On the basis of the phylogenetic tree of the selected UGT isoforms constructed by the Neighbor-Joining-method (Supplemental Fig. 1), mouse Ugt2b36 is suggested to branch from a common ancestor of guinea pig UGT2B21, another morphine conjugating UGT. Also, mouse Ugt2b1 has been considered as an orthologue of rat UGT2B1 (Mackenzie, 1987; Mackenzie et al., 2005) which catalyzes morphine glucuronidation (Prichard et al., 1994). Furthermore, this is also supported by the phylogenetic tree in this study (Supplemental Fig. 1). It is reasonable to suppose that mouse Ugt2b1 and rat UGT2B1 are orthologues. However, mouse Ugt2b1 did not show any substantial activity toward morphine (Fig. 4). Therefore, care should be taken in discussing the function of Ugt isoforms, especially a candidate orthologue such as mouse Ugt2b1 prior to characterizing function. For human UGT2B7, it has been shown that Asp99 is important for the binding of morphine (Coffman et al., 2003). In rat UGT2B1, the residue is conserved as Asp100 while it was substituted to Glu100 in mouse Ugt2b1. Of the other UGT isoforms catalyzing morphine glucuronidation, guinea pig UGT2B21 (Ishii et al., 2001) and mouse Ugt2b36 have Thr98 and Glu100 at the corresponding position, respectively. Although mouse Ugt2b36 carries the acidic amino-acid Glu instead of Asp, it is unlikely to be definitive for the catalysis of morphine glucuronidation. The amino acid identity of mouse Ugt2b1 and rat UGT2B1 is 86%

and there are 37 amino-acid differences between them. Therefore, it is assumed that these differences resulted in the different substrate specificity of mouse Ugt2b1 from rat UGT2B1. The amino acids sequences in the N-terminal half of UGTs have been considered to be important for substrate binding. However, the details remain to be clarified.

Data from the kinetic analysis showed that the Km of mouse Ugt2b36 is lower than that of UGT2B7 which is a predominant UGT catalyzing morphine glucuronidation in human liver. Thus, it seems that Ugt2b36 exhibits higher affinity for morphine than UGT2B7. Furthermore, the Vmax of Ugt2b36 was approximately 5-times higher than that of UGT2B7. Thus, the intrinsic clearance of Ugt2b36 was 17-times higher than that of UGT2B7. However, the expression level of UGT2B7 in Sf9 microsomes used in this study has not been accurately determined. The Km of UGT2B7 in COS cell microsomes (Takeda et al., 2005) was comparable with that of Ugt2b36 in this study. This suggests that Ugt2b36 exhibits higher glucuronidation activity toward morphine than UGT2B7. However, since there are differences in the expression systems, we cannot conclude that there are definitive differences. Also, there is a report that the relative morphine-glucuronidation activities of human liver microsomes (HLM) and MLM were 1 : 64 (Higashi et al., 2014). Therefore, this strongly suggests that both Ugt2b36 and UGT2B7 are predominant UGT isoforms in mouse and human livers, respectively. Mouse Ugt2b36 is mainly expressed in the liver but the level is quite low in other tissues (Buckley and Klaassen, 2007). The hepatic ontogeny of Ugt mRNA of mice has been reported (Lu et al., 2013). Mouse Ugt2b36 is expressed as one of the major isoforms in the fetus, then reduced at birth, but increased to be a predominant isoform again in the liver at puberty and in adulthood (Lu et al., 2013). Taking these findings into consideration, mouse Ugt2b36 is a predominant isoform

participating in morphine glucuronidation in the liver.

There were multiple bands in the Ugt2b35 preparation examined in this study while the other Ugts examined in this study were expressed as an apparent single band (Fig. 1A). Therefore, we carried out the EndoH digestion on Ugt2b35 (Supplemental Fig. 2) to determine the cause of this multiple banding. It is evident that Ugt2b35 in the preparation is glycosylated. There are three potential N-glycosylation-sites in Ugt2b35. The lower and higher bands (Fig. 1A) are probably differently glycosylated forms. Ugt2b35 exhibited considerable activity toward the universal substrate 4-MU. Since the Ugt2b35 preparation used in this study consisted of a relatively high amount of the lesser glycosylated form, we cannot exclude the possibility that the multiple-glycosylated form shows higher activity. In addition, glycosylation of Ugt2b36 was not obvious (Supplemental Fig. 2). We carried out the expression of Ugt carefully and most Ugt isoforms except Ugt2b35 are expressed as a single band on SDS-PAGE gels. A previous report suggested that transfection with high amounts of virus results in the production of inactive UGT (Zhang et al., 2012). In consideration of this, we used low MOI and the shorter durations of transfection so that it is reasonable to suppose that the Ugt isoforms examined in this study are expressed properly as demonstrated by their substantial glucuronidation activity toward the universal substrate 4-MU. Again, Ugt2b37 also exhibits substantial activity toward 4-MU. Better substrates for Ugt2b35 and 2b37 are yet to be identified.

Regarding estradiol glucuronidation, glucuronidation at the 3-hydroxyl group is seen as a marker activity of human UGT1A1 (Senafi et al., 1994; Court 2005). Similarly, in mice, Ugt1a1 exhibits high activity at the 3-hydroxyl position of estradiol but not at the 17-hydroxyl group (Figs. 3 and 6). Glucuronidation at the 17-hydroxyl group was also catalyzed by Ugt2b1, 2b5,

2a3, 2b34, 2b35 and 2b38 (Fig. 3). However, Ugt2a3, 2b34, 2b35 and 2b38 did not exhibit any significant activity at the lower concentration (10 μM). This suggests that Ugt2b5 and 2b1 are important under physiological conditions. In humans, UGT2B15 and 2B17 are predominant catalysts of 17β-hydroxysteroid glucuronidation (Beaulieu et al., 1996). Therefore, it is reasonable to suppose that, in mice, Ugt2b1 and 2b5 are functional orthologues of human UGT2B15 and 2B17. Also, mouse Ugt2b1 and 2b5 are the major isoforms expressed in adults (Lu et al., 2013). Therefore, mouse Ugt2b1 and 2b5 seem to play important roles in the glucuronidation of 17β-hydroxysteroids in the adult.

Ugt2b1 and 2b5 exclusively catalyze chloramphenicol glucuronidation (Fig. 4B) while the other isoforms examined did not. Chloramphenicol is known to be a substrate for rat UGT2B1 (Mackenzie, 1987). Therefore, the substrate specificity of Ugt2b1 was somewhat conserved for chloramphenicol glucuronidation. Also, a high level of Ugt2b5 is expressed in the fetus and in newborn, and the expression of Ugt2b1 is very low at the fetal and new born stages (Lu et al., 2013). However, both Ugt2b1 and 2b5 are significantly expressed in the adult mouse liver (Lu et al., 2013). Although both Ugt2b1 and 2b5 exhibit similar substrate specificity (Figs. 3 and 4B), further studies are necessary to clarify why they are differently regulated during the developmental stages.

Although the catalytic properties of other substrates are also important, this study provides a comprehensive characterization of Ugt2b subfamily isoforms in mice using typical substrates. The data obtained suggest that Ugt2b36 is a predominant isoform involved in morphine glucuronidation in mouse liver. Furthermore, typical isoforms involved in estradiol and chloramphenicol glucuronidation were identified. Further studies are necessary to interpret the

stress- and chemical-induced changes in glucuronidation activity and the expression levels of Ugt isoforms in mouse liver.

Acknowledgements

The authors thank the Research Support Center, Research Center for Human Disease Modeling, Graduate School of Medical Sciences, Kyushu University, for technical support.

Authorship Contributions

Participated in research design: Kurita, Miyauchi, Mackenzie, Yamada, Ishii

Conducted experiments: Kurita, Miyauchi, Ishii

Contributed new reagents or analytical tools: Kurita, Miyauchi, Ikushiro

Performed data analysis: Kurita, Miyauchi, Ishii

Wrote or contributed the writing of the manuscript: Kurita, Mackenzie, Ishii

References

Beaulieu M, Lévesque E, Hum DW, and Bélanger A (1996) Isolation and characterization of a novel cDNA encoding a human UDP-glucuronosyltransferase active on C19 steroids. *J Biol Chem* **271**: 22855-22862.

Buckley DB and Klaassen CD (2007) Tissue- and gender-specific mRNA expression of UDP-glucuronosyltransferases (UGTs) in mice. *Drug Metab Dispos* **35**: 121–127.

Buckley DB and Klaassen CD (2009a) Mechanism of gender-divergent UDP-glucuronosyltransferase mRNA expression in mouse liver and kidney. *Drug Metab Dispos* **37**: 834–840.

Buckley DB and Klaassen CD (2009b). Induction of mouse UDP-glucuronosyltransferase mRNA expression in liver and intestine by activators of aryl-hydrocarbon receptor, constitutive androstane receptor, pregnane X receptor, peroxisome proliferator-activated receptor alpha, and nuclear factor erythroid 2-related factor 2. *Drug Metab Dispos* **37**: 847-856.

Coffman BL, Kearney WR, Goldsmith S, Knosp BM, and Tephly TR (2003) Opioids bind to the amino acids 84 to 118 of UDP-glucuronosyltransferase UGT2B7. *Mol Pharmacol* **63**: 283–288.

Coffman BL, Rios GR, King CD, and Tephly TR (1997) Human UGT2B7 catalyzes morphine glucuronidation. *Drug Metab Dispos* **25**: 1–4.

Court MH (2005) Isoform-selective probe substrates for in vitro studies of human UDP-glucuronosyltransferases. *Methods Enzymol* **400**: 104-116.

Court MH, Hazarika S, Krishnaswamy S, Finel M, and Williams JA (2008) Novel polymorphic human UDP-glucuronosyltransferase 2A3: cloning, functional characterization of enzyme variants, comparative tissue expression, and gene induction. *Mol Pharmacol* **74**: 744-754.

Evans WE and Relling MV (1999) Pharmacogenomics: translating functional genomics into rational therapeutics. *Science* **286**: 487–491.

Guengerich FP (2006) Cytochrome P450s and other enzymes in drug metabolism and toxicity. *AAPS J* **8**: E101-E111.

Fay MJ, Nguyen MT, Snouwaert JN, Dye R, Grant DJ, Bodnar WM, and Koller BH (2015) Xenobiotic Metabolism in Mice Lacking the UDP-Glucuronosyltransferase 2 Family. *Drug Metab Dispos* **43**: 1838-1846.

Higashi E, Ando A, Iwano S, Murayama M, and Yamazaki H (2014) Hepatic microsomal UDP-glucuronosyltransferase (UGT) activities in the microminipig. *Biopharm Drug Dispos* **35**: 313–320.

Ishii Y, Miyoshi A, Watanabe R, Tsuruda K, Tsuda M, Yamaguchi-Nagamatsu Y, Yoshisue K, Tanaka M, Maji D, Ohgiya S, and Oguri K (2001) Simultaneous expression of guinea pig UDP-glucuronosyltransferase 2B21 and 2B22 in COS-7 cells enhances UDP-glucuronosyltransferase 2B21-catalyzed morphine-6-glucuronide formation. *Mol Pharmacol* **60**: 1040–1048.

Ishii Y, Koba H, Kinoshita K, Oizaki T, Iwamoto Y, Takeda S, Miyauchi Y, Nishimura Y, Egoshi N, Taura F, Morimoto S, Ikushiro S, Nagata K, Yamazoe Y, Mackenzie PI, and Yamada H (2014) Alteration of the function of the UDP-glucuronosyltransferase 1A subfamily by cytochrome P450 3A4: different susceptibility for UGT isoforms and UGT1A1/7 variants. *Drug Metab Dispos* **42**: 229-238.

Iyanagi T (1991) Molecular basis of multiple UDP-glucuronosyltransferase isoenzyme deficiencies in the hyperbilirubinemic rat (Gunn rat). *J Biol Chem* **266**: 24048-24052.

Jin CJ, Miners JO, Lillywhite KJ, and Mackenzie PI (1993). cDNA cloning and expression of two new members of the human liver UDP-glucuronosyltransferase 2B subfamily. *Biochem Biophys Res Commun* **194**: 496-503.

Kasai N, Sakaki T, Shinkyo R, Ikushiro S, Iyanagi T, Kamao M, Okano T, Ohta M, Inouye K. (2004) Sequential metabolism of 2,3,7-trichlorodibenzo-p-dioxin (2,3,7-triCDD) by cytochrome P450 and UDP-glucuronosyltransferase in human liver microsomes. Drug Metab Dispos. **32**: 870-875.

Kato Y, Haraguchi K, Shibahara T, Shinmura Y, Masuda Y, and Kimura R (2000) The induction of hepatic microsomal UDP-glucuronosyltransferase by the methylsulfonyl metabolites of polychlorinated biphenyl congeners in rats. *Chem Biol Interact* **125**: 107-115.

Kimura T and Owens IS (1987) Mouse UDP glucuronosyltransferase. cDNA and complete amino acid sequence and regulation. *Eur J Biochem* **168**: 515-521.

Kong AN, Ma M, Tao D, and Yang L (1993) Molecular cloning of two cDNAs encoding the mouse bilirubin/phenol family of UDP-glucuronosyltransferases (mUGTBr/p). *Pharm Res* **10**: 461–465.

Kuo CK, Hanioka N, Hoshikawa Y, Oguri K, and Yoshimura H (1991) Species difference of site-selective glucuronidation of morphine. *J Pharmacobiodyn* **14**: 187–193.

Lévesque E, Turgeon D, Carrier JS, Montminy V, Beaulieu M, and Bélanger A (2001) Isolation and characterization of the UGT2B28 cDNA encoding a novel human steroid conjugating UDP-glucuronosyltransferase. *Biochemistry* **40**: 3869-3881.

Lu H, Gonzalez FJ, and Klaassen C (2010) Alterations in hepatic mRNA expression of phase II enzymes and xenobiotic transporters after targeted disruption of hepatocyte nuclear factor 4

alpha. *Toxicol Sci* **118**: 380-390.

Lu H, Gunewardena S, Cui JY, Yoo B, Zhong XB, and Klaassen CD (2013) RNA-sequencing quantification of hepatic ontogeny and tissue distribution of mRNAs of phase II enzymes in mice. *Drug Metab Dispos* **41**: 844-857.

Lowry OH, Rosebrough NJ, Farr AL, and Randall RJ (1951) Protein measurement with the Folin phenol reagent. *J Biol Chem* **193**: 265–275.

Mackenzie PI, Hjelmeland LM, and Owens IS (1984) Purification and immunochemical characterization of a low-pI form of UDP glucuronosyltransferase from mouse liver. *Arch Biochem Biophys* **231**: 487–497.

Mackenzie PI (1987) Rat liver UDP-glucuronosyltransferase. Identification of cDNAs encoding two enzymes which glucuronidate testosterone, dihydrotestosterone, and beta-estradiol. *J Biol Chem* **262**: 9744-9749.

Mackenzie PI, Bock KW, Burchell B, Guillemette C, Ikushiro S, Iyanagi T, Miners JO, Owens IS, and Nebert DW (2005) Nomenclature update for the mammalian UDP glycosyltransferase (UGT) gene superfamily. *Pharmacogenet Genomics* **15**: 677–685.

Miyauchi Y, Nagata K, Yamazoe Y, Mackenzie PI, Yamada H and Ishii Y (2015) Suppression of Cytochrome P450 3A4 Function by UDP-Glucuronosyltransferase 2B7 through a Protein-Protein Interaction: Cooperative Roles of the Cytosolic Carboxyl-Terminal Domain and the Luminal Anchoring Region. *Mol Pharmacol* **88**: 800-812.

Nakamura T, Yamaguchi N, Miyauchi Y, Takeda T, Yamazoe Y, Nagata K, Mackenzie PI, Yamada H, Ishii Y (2016) Introduction of an N-Glycosylation Site into UDP-Glucuronosyltransferase 2B3 Alters Its Sensitivity to Cytochrome P450 3A1-Dependent

Modulation. *Front Pharmacol* **7**: 427.

Nguyen N, Bonzo JA, Chen S, Chouinard S, Kelner MJ, Hardiman G, Bélanger A, and Tukey RH (2008) Disruption of the ugt1 locus in mice resembles human Crigler-Najjar type I disease. *J Biol Chem* **283**: 7901-7911.

Nishimura Y, Maeda S, Ikushiro S, Mackenzie PI, Ishii Y, and Yamada H (2007) Inhibitory effects of adenine nucleotides and related substances on UDP-glucuronosyltransferase: structure-effect relationships and evidence for an allosteric mechanism. *Biochim Biophys Acta* **1770**: 1557–1566.

Nurrochmad A, Ishii Y, Nakanoh H, Inoue T, Horie T, Sugihara K, Ohta S, Taketomi A, Maehara Y, and Yamada H (2010) Activation of morphine glucuronidation by fatty acyl-CoAs and its plasticity: a comparative study in humans and rodents including chimeric mice carrying human liver. *Drug Metab Pharmacokinet* **25**: 262–273.

Oguri K, Ida S, Yoshimura H, and Tsukamoto H (1970) Metabolism of drugs. LXIX. Studies on the urinary metabolites of morphine in several mammlian species. *Chem Pharm Bull (Tokyo)* **18**: 2414–2419.

Oguri K, Kurogi A, Yamabe K, Tanaka M, Yoshisue K, Ishii Y, and Yoshimura H (1996) Purification of a phenobarbital-inducible UDP-glucuronosyltransferase isoform from dog liver which catalyzes morphine and testosterone glucuronidation. *Arch Biochem Biophys* **325**: 159-166.

Okie S (2010) A flood of opioids, a rising tide of deaths. *N Engl J Med* **363**: 1981–1985.

Pritchard M, Fournel-Gigleux S, Siest G, Mackenzie P, and Magdalou J (1994) A recombinant phenobarbital-inducible rat liver UDP-glucuronosyltransferase (UDP-glucuronosyltransferase

2B1) stably expressed in V79 cells catalyzes the glucuronidation of morphine, phenols, and carboxylic acids. *Mol Pharmacol* **45**: 42–50.

Ritter JK, Sheen YY, and Owens IS (1990) Cloning and expression of human liver UDP-glucuronosyltransferase in COS-1 cells. 3,4-catechol estrogens and estriol as primary substrates. *J Biol Chem* **265**: 7900-7906.

Ritter JK, Crawford JM, and Owens IS (1991) Cloning of two human liver bilirubin UDP-glucuronosyltransferase cDNAs with expression in COS-1 cells. *J Biol Chem* **266**: 1043-1047.

Ritter JK, Chen F, Sheen YY, Tran HM, Kimura S, Yeatman MT, and Owens IS (1992) A novel complex locus UGT1 encodes human bilirubin, phenol, and other UDP-glucuronosyltransferase isozymes with identical carboxyl termini. *J Biol Chem* **267**: 3257-3261.

Saitou N and Nei M (1987) The neighbor-joining method: a new method for reconstructing phylogenetic trees. *Mol Biol Evol* **4**: 406–425.

Senafi SB, Clarke DJ, and Burchell B (1994) Investigation of the substrate specificity of a cloned expressed human bilirubin UDP-glucuronosyltransferase: UDP-sugar specificity and involvement in steroid and xenobiotic glucuronidation. *Biochem J* **303**: 233–240.

Shimomura K, Kamata O, Ueki S, Iida S, Oguri K, Yoshimura H, and Tsukamoto H (1971) Analgesic effect of morphine glucuronides. *Tohoku J Exp Med* **105**: 45–52.

Stone AN, Mackenzie PI, Galetin A, Houston JB, and Miners JO (2003) Isoform selectivity and kinetics of morphine 3- and 6-glucuronidation by human udp-glucuronosyltransferases: evidence for atypical glucuronidation kinetics by UGT2B7. *Drug Metab Dispos* **31**: 1086–1089.

Svensson JO, Rane A, Säwe J, and Sjöqvist F (1982) Determination of morphine,

morphine-3-glucuronide and (tentatively) morphine-6-glucuronide in plasma and urine using ion-pair high-performance liquid chromatography. *J Chromatogr* **230**: 427–432.

Takeda S, Ishii Y, Iwanaga M, Mackenzie PI, Nagata K, Yamazoe Y, Oguri K, and Yamada H (2005) Modulation of UDP-glucuronosyltransferase function by cytochrome P450: evidence for the alteration of UGT2B7-catalyzed glucuronidation of morphine by CYP3A4. *Mol Pharmacol* **67**: 665–672.

Uchihashi S, Nishikawa M, Sakaki T, and Ikushiro S (2012) The critical role of amino acid residue at position 117 of mouse UDP-glucuronosyltransfererase 1a6a and 1a6b in resveratrol glucuronidation. *J Biochem* **152**: 331–340.

Uchihashi S, Nishikawa M, Sakaki T, and Ikushiro S (2013) Comparison of serotonin glucuronidation activity of UDP-glucuronosyltransferase 1a6a (Ugt1a6a) and Ugt1a6b: evidence for the preferential expression of Ugt1a6a in the mouse brain. *Drug Metab Pharmacokinet* **28**: 260–264.

Williams JA, Hyland R, Jones BC, Smith DA, Hurst S, Goosen TC, Peterkin V, Koup JR, and Ball SE (2004) Drug-drug interactions for UDP-glucuronosyltransferase substrates: a pharmacokinetic explanation for typically observed low exposure (AUCi/AUC) ratios. *Drug Metab Dispos* **32**: 1201–1208.

World Health Organization (1996) Cancer pain relief with a guide to opioid availability (2nd ED.), Ganeva, Switzerland, WHO

Yoshimura H, Oguri K, and Tsukamoto H (1968) Metabolism of drugs. LX. The synthesis of codeine and morphine glucuronides. *Chem Pharm Bull (Tokyo)* **16**: 2114-2119.

Yoshimura H, Oguri K, and Tsukamoto H (1969) Metabolism of drugs. LXII. Isolation and

identification of morphine glucuronides in urine and bile of rabbits. *Biochem Pharmacol* **18**: 279–286.

Zhang H, Patana AS, Mackenzie PI, Ikushiro S, Goldman A, Finel M (2012) Human UDP-glucuronosyltransferase expression in insect cells: ratio of active to inactive recombinant proteins and the effects of a C-terminal his-tag on glucuronidation kinetics. *Drug Metab Dispos* **40**: 1935-1944.

Footnotes

This study was supported in part by Grants-in-Aid for Scientific Research (B)[#25293039] and Challenging Exploratory Research [#16K15148] from the Japanese Society for the Promotion of Science to Y.I.

Presented in part at:

The international Conjugation Workshop 2016, Vancouver, Canada, June, 2016 (Ishii et al);

135th Annual meeting of the Pharmaceutical Society of Japan, Kobe, Japan, March 2015 (Kurita et al); 30th Annual meeting of the Japanese Society of the Study of Xenobiotics, Tokyo, Japan, November 2015 (Kurita et al)

[1]Deceased

To whom correspondence should be addressed:

Yuji Ishii, Ph.D. Graduate School of Pharmaceutical Sciences, Kyushu University, 3-1-1 Maidashi, Higashi-ku, Fukuoka 812-8582, JAPAN

Phone: +81-92-642-6586

Fax: +81-92-642-6588

E-mail: ishii@phar.kyushu-u.ac.jp

Figure Legends

Fig. 1. Immunoblots of the expression of Ugt1a1, 2a3 and all the Ugt2b subfamily isoforms in Sf-9 cells by an antibody toward a mouse low-p*I* form Ugt (A) and anti-UGT2B antibody (B).

To obtain microsomes expressing each mouse Ugt, Sf-9 cells were transfected with recombinant baculovirus for the corresponding Ugt isoform. In (A), the lane labeled shows the microsomal samples of the transfected cells. Baculosomes (5 μg protein) from Ugt expressing cells were electrophoresed (10% SDS-PAGE) and electrophoretically transferred to PVDF membrane. Then, Ugts were detected by anti-mouse low-p*I* form UGT antibody (Mackenzie et al., 1984) as the primary antibody. Pooled MLM (n=5, 10 μg protein) was used as a positive control. Mock represents microsomes obtained from Sf9 cells transfected with control baculovirus. In (B), the lane labeled shows the microsomal samples of the transfected cells. Baculosomes (10 μg protein) from Ugt2b5-expressing Sf-9 cells were electrophoresed (7.5% SDS-PAGE). For other baculosomes, amounts of protein were used that were comparable to the Ugt content in the Ugt2b5. For Ugt2b35, the sample was treated with EndoH according to Nakamura et al. (2016) prior to subject to the SDS-PAGE. Then, those were electrophoretically transferred to PVDF membrane. Ugts were detected by anti-UGT2B antibody (Kasai et al., 2004) as the primary antibody. Details are described in Materials and Methods.

Fig. 2. Comparison of the glucuronidation activity of each mouse Ugt isoform toward

4-methylumbelliferone

Baculosomes (100 μg protein) from each Ugt single-expressing Sf-9 cell were used. The concentrations of 4-MU and UDPGA were fixed at 200 μM and 2 mM, respectively. Each bar represents the mean ± S.D. of a triplicate assay. The activity was calculated based on the relative Ugt level and then normalized to the Ugt level by Ugt2b36-expressing microsomes. Details are described in Materials and Methods.

Fig. 3. Comparison of the glucuronidation activity of each mouse Ugt isoform toward 17β-estradiol

Baculosomes (100 μg protein) from each Ugt single-expressing Sf-9 cell were used. The concentrations of 17β-estradiol were fixed at 1 mM (A, B) and 10 μM (C), respectively. UDPGA was fixed at 2 mM. E3G and E17G formed were simultaneously determined by HPLC. In (A), E3G and E17G activities are shown in a same scale. In (B), E17G activity in (A) is shown in an enlarged scale. In (C), E17G activity at the low substrate (10 μM) is shown. Each bar represents the mean ± S.D. of a triplicate assay. The activity was normalized as described in the legend to Fig. 2. Details are described in Materials and Methods.

Fig. 4. Comparison of the glucuronidation activity of each mouse Ugt isoform toward morphine and chloramphenicol

Baculosomes (200 μg protein) from each Ugt single-expressing Sf-9 cell were used. The concentrations of morphine and chloramphenicol used were 5 mM. The UDPGA concentration was fixed at 2 mM. Formation of M-3-G (A) and chloramphenicol glucuronide (B) were

determined by HPLC. Each bar represents the mean ± S.D. of a triplicate assay. The activity was normalized as described in the legend to Fig. 2. Details are described in Materials and Methods.

Fig. 5. Comparison of Michaels-Menten plots of morphine-3-glucuronidation activity among MLM, Sf9 microsomes expressing mouse Ugt2b36 and human UGT2B7

Morphine-3-glucuronidation activity was compared among MLM (A), microsomes expressing Ugt2b36 (B) and UGT2B7 (C). Baculosomes (100 μg protein) from each Ugt-expressing Sf-9 cell or MLM were used. Each plot represents the mean ± S.D. of a triplicate assay. Data were fitted to a Michaelis-Menten equation or a sigmoidal equation. The morphine concentrations ranged from 0.1 to 6 mM. The kinetic parameters obtained are listed in Table 2.

Fig. 6. Comparison of Michaels-Menten plots of estradiol-3-glucuronidation activity between MLM and Sf9 microsomes expressing mouse Ugt1a1

E3G activity was compared between MLM (A) and microsomes expressing Ugt1a1 (B). MLM (100 μg protein) or baculosomes (100 μg protein) from Ugt1a1-expressing Sf-9 cell were used. Each plot represents the mean ± S.D. of a triplicate assay. Data were fitted to a Michaelis-Menten equation. The 17β-estradiol concentrations ranged from 1 to 100 μM. The kinetic parameters obtained are listed in Table 3.

JPET Fast Forward. Published on February 22, 2017 as DOI: 10.1124/jpet.117.240382
This article has not been copyedited and formatted. The final version may differ from this version.

Table 1 Primers used for amplification of Ugt cDNA from mouse liver

Each Ugt cDNA was amplified using the oligo-dT primed cDNA as a template that was reverse-transcribed from mouse liver total-RNA (1st round PCR). Nested PCR was carried out using two sets of primer pairs. For the 1st round PCR, a primer pair without a restriction site was used. For the second round PCR (nested PCR), each Ugt cDNA was amplified with a primer pair with a restriction site. Single and double underlines represent *Not*I and *Xho*I sites, respectively.

Target		Sequences
Ugt1a1	Forward (1st)	5-GCAGCATCAGAGAGAGAGAGATACC-3’
	Reverse (1st)	5’-CAACTGATCAGATAATGAACTAATACTTCTCC-3’
	Forward (2nd)	5’-ATAAGAATGCGGCCGCGCCATGACTGTGGTGTGCTGG-3’
	Reverse (2nd)	5’-CCGCTCGAGTCAATGGGTCTTGGATTTGTGTGATTTC-3’
Ugt2a3	Forward (1st)	5’-GCGAAACAACTTGAGGAGGCAC-3’
	Reverse (1st)	5’-TAATTGTCACTCAGGGCTTTCCC-3’
	Forward (2nd)	5’-ATAAGAATGCGGCCGCGATATGGTCTCTGAAAAATGTGTTGCG-3’
	Reverse (2nd)	5’-CCGCTCGAGGGCTTTCCCAAACCTAAAAAAGACCTAG-3’
Ugt2b1	Forward (1st)	5’-GCAAGATGTCTATGAAACAGGCTTC-3’
	Reverse (1st)	5’-ACTCTCTGCTTCAGCCTTCATGAAG-3’
	Forward (2nd)	5’-ATAAGAATGCGGCCGCGAGATGTCTATGAAACAGGCTTCAG-3’
	Reverse (2nd)	5’-CCGCTCGAGCTACTCTTTTTTCTTCTTTCCCATGTTAGC-3’
Ugt2b5	Forward (1st)	5’-CTGTGAGAGAAGGATTTTGATTTTCAAGATGC-3’
	Reverse (1st)	5’-TTGTTCATGTAGTTCATTGTCAGTGAGC-3’
	Forward (2nd)	5’-ATAAGAATGCGGCCGCGAGATGCCTGGAAAGTGGATTTCTG-3’
	Reverse (2nd)	5’-CCGCTCGAGCTACTCATTCTTCATTTTATTTTCTTTCTTTACAAAGAATC-3’
Ugt2b34	Forward (1st)	5’-GCCTGAAGTTAACCAAGATGCCTG-3’
	Reverse (1st)	5’-TGGAAAGGACCATGTGTCAGTCTTC-3’
	Forward (2nd)	5’-ATAAGAATGCGGCCGCGAGATGCCTGTGAAAATGACAGC-3’

JPET Fast Forward. Published on February 22, 2017 as DOI: 10.1124/jpet.117.240382
This article has not been copyedited and formatted. The final version may differ from this version.

	Reverse	(2nd)	5’-CCGCTCGAGGTCAGTCTTCCCCAGTTCAGCTAC-3’
Ugt2b35	Forward	(1^{st})	5’-AACAGAAGCCCTTTGACTTCCAGG-3’
	Reverse	(1^{st})	5’-AATGCTGAAGTTTCATTCATGTAGTGC-3’
	Forward	(2nd)	5’-ATAAGAATGCGGCCGCGGGATGCCTGTGAAGTGG-3’
	Reverse	(2nd)	5’-CCGCTCGAGCATGTAGTGCATTGTCAATGAGCTCTAC-3’
Ugt2b36	Forward	(1^{st})	5’-GAAGAACATTGATTTTCAGAATGCTTTGG-3’
	Reverse	(1^{st})	5’-ATTCATGTAATGCATTATCAATGAGTTCTACTC-3’
	Forward	(2nd)	5’-ATAAGAATGCGGCCGCGGAATGCTTTGGAAGTGGATTTCTG-3’
	Reverse	(2nd)	5’-CCGCTCGAGCTACTCATTCTTCATTTTCTTTTCTTTCTTTACAAAGAATC-3’
Ugt2b37	Forward	(1^{st})	5’-AGGATTTTGATTTTCAGGATGCCTG-3’
	Reverse	(1^{st})	5’-GAGGCTGAAAGTTCATTCATGTGG-3’
	Forward	(2nd)	5’-ATAAGAATGCGGCCGCGGGATGCCTGGAAAGTGG-3’
	Reverse	(2nd)	5’-CCGCTCGAGGTGGTGCATTGACAATGAACTCTAC-3’
Ugt2b38	Forward	(1^{st})	5’-CTGTGAAGAGAAGGATTTTGATTTTCAGG-3’
	Reverse	(1^{st})	5’-GAATGAGGGTGAAAGTTCATTCATG-3’
	Forward	(2nd)	5’-ATAAGAATGCGGCCGCGGGATGCCTGGAAAGTGGATTTC-3’
	Reverse	(2nd)	5’-CCGCTCGAGGTAGTCCATTGTCAATGAGCTCTACTCATTC-3’

JPET Fast Forward. Published on February 22, 2017 as DOI: 10.1124/jpet.117.240382
This article has not been copyedited and formatted. The final version may differ from this version.

Table 2 Kinetic parameters for morphine-3-glucuronidation catalyzed by MLM, microsomes of Sf9-cells expressing Ugt2b36 and UGT2B7: kinetics by varying the morphine concentration

Isoforms	Vmax (nmol/min/mg protein)	Km (mM)	Hill coefficient (n)	CLint (μL/min/mg protein)
MLM	4.72 ± 0.14	0.39 ± 0.05	-	12.1
Ugt2b36	1.08 ± 0.03	0.24 ± 0.04	-	4.56
UGT2B7	0.23 ± 0.01	0.88 ± 0.06	2.65 ± 0.38	0.26

Data were fitted to a Michaelis-Menten equation or a sigmoidal equation (Fig. 4). Results are the estimated value ± S.E.

JPET Fast Forward. Published on February 22, 2017 as DOI: 10.1124/jpet.117.240382
This article has not been copyedited and formatted. The final version may differ from this version.

Table 3 Kinetic parameters for estradiol-3-glucuronidation catalyzed by MLM and microsomes of Sf9-cells expressing Ugt1a1: kinetics by varying 17β-estradiol

Isoforms	Vmax (pmol/min/mg protein)	Km (μM)
MLM	556.1 ± 25.2	17.5 ± 2.3
Ugt1a1	61.1 ± 5.40	3.18 ± 1.10

Data were fitted to a Michaelis-Menten equation (Fig. 6). Results are the estimated value ± S.E.

JPET Fast Forward. Published on February 22, 2017 as DOI: 10.1124/jpet.117.240382
This article has not been copyedited and formatted. The final version may differ from this version.

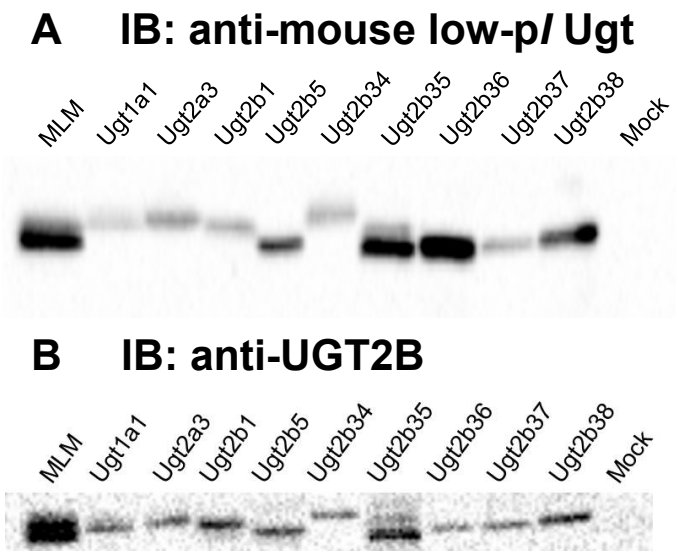

Kurita et al, Fig. 1

JPET Fast Forward. Published on February 22, 2017 as DOI: 10.1124/jpet.117.240382
This article has not been copyedited and formatted. The final version may differ from this version.

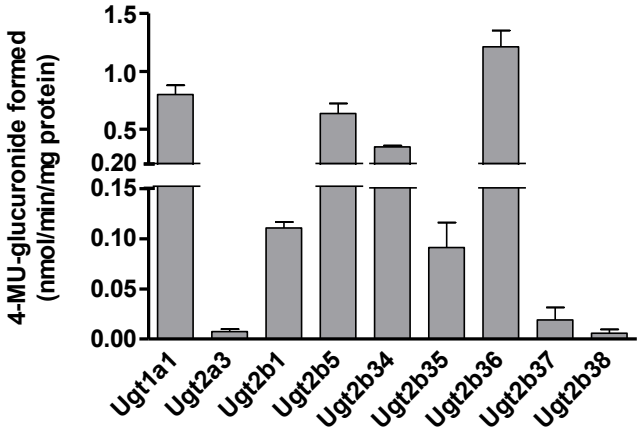

Kurita et al, Fig. 2

JPET Fast Forward. Published on February 22, 2017 as DOI: 10.1124/jpet.117.240382
This article has not been copyedited and formatted. The final version may differ from this version.

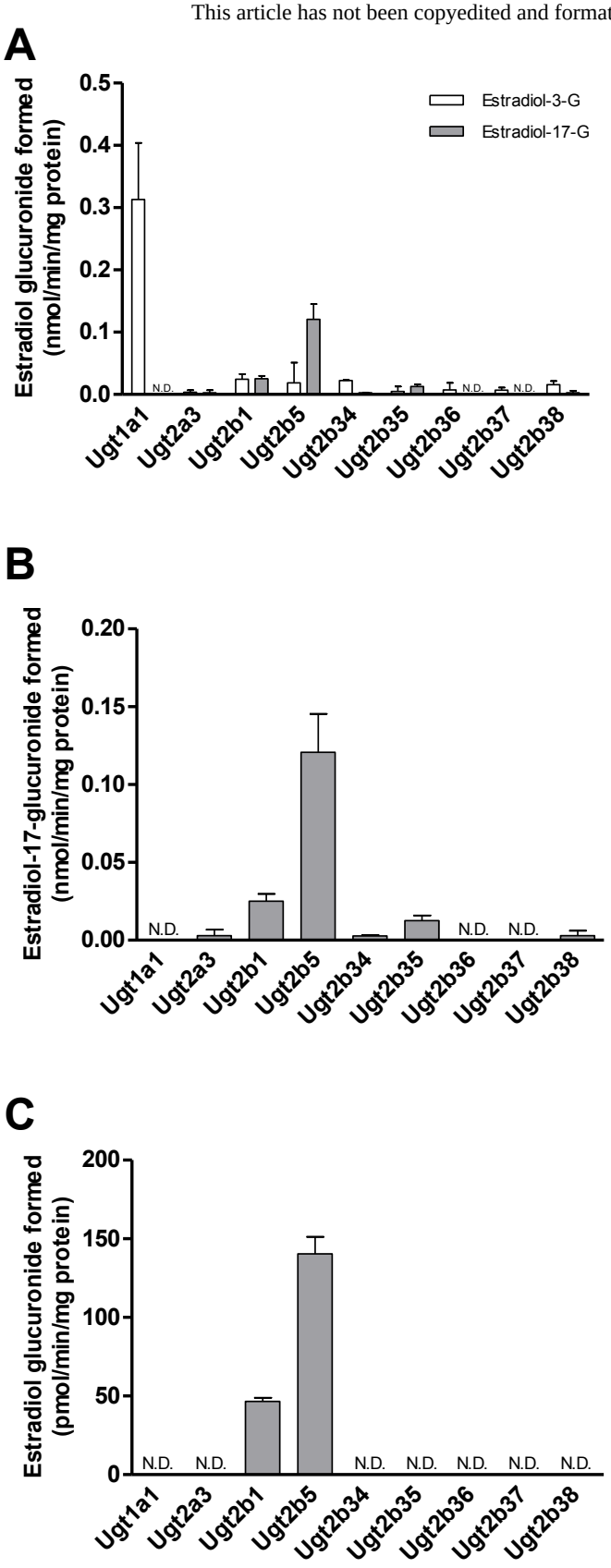

Kurita et al, Fig. 3

JPET Fast Forward. Published on February 22, 2017 as DOI: 10.1124/jpet.117.240382
This article has not been copyedited and formatted. The final version may differ from this version.

A

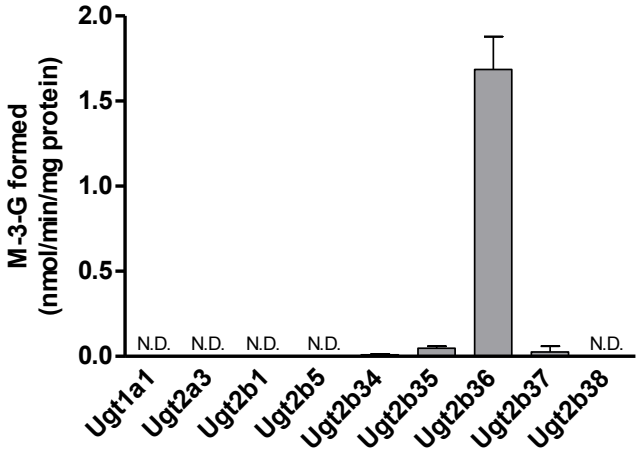

B

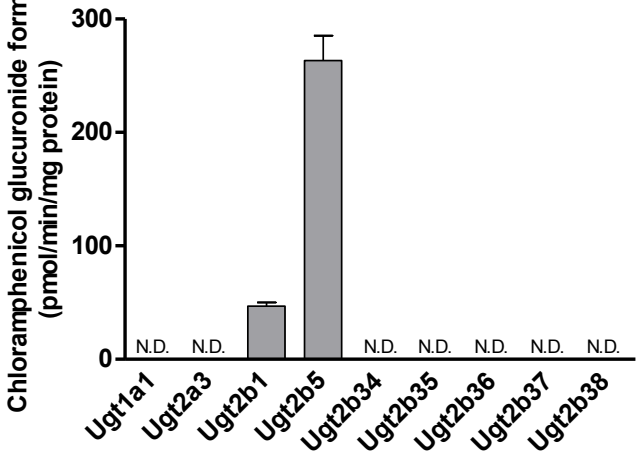

Kurita et al, Fig. 4

JPET Fast Forward. Published on February 22, 2017 as DOI: 10.1124/jpet.117.240382
This article has not been copyedited and formatted. The final version may differ from this version.

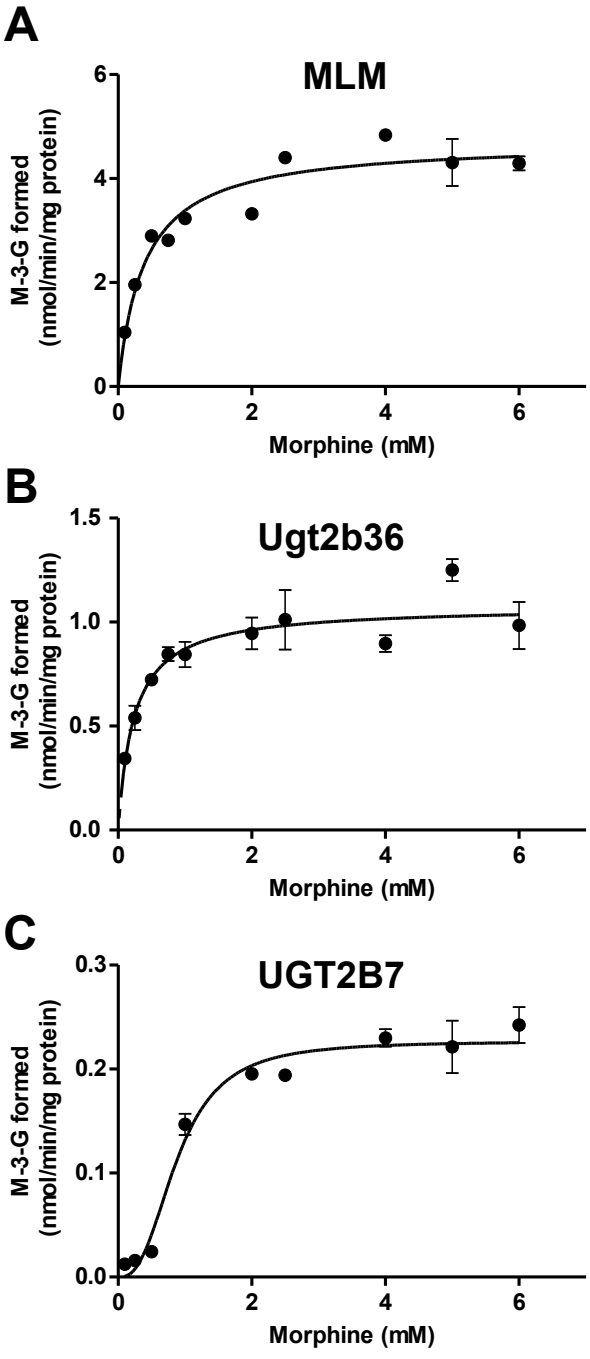

Kurita et al, Fig. 5

JPET Fast Forward. Published on February 22, 2017 as DOI: 10.1124/jpet.117.240382
This article has not been copyedited and formatted. The final version may differ from this version.

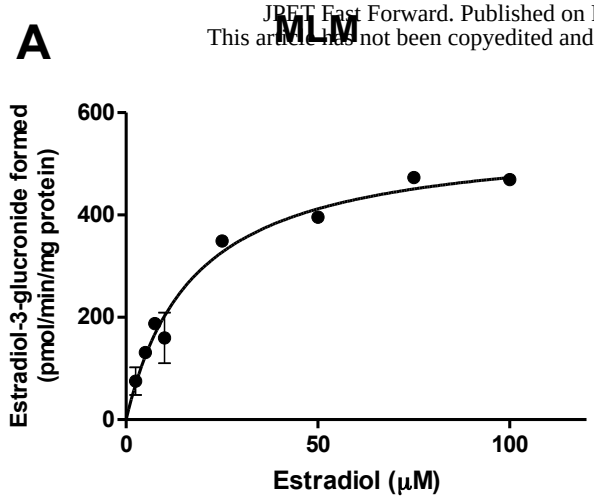

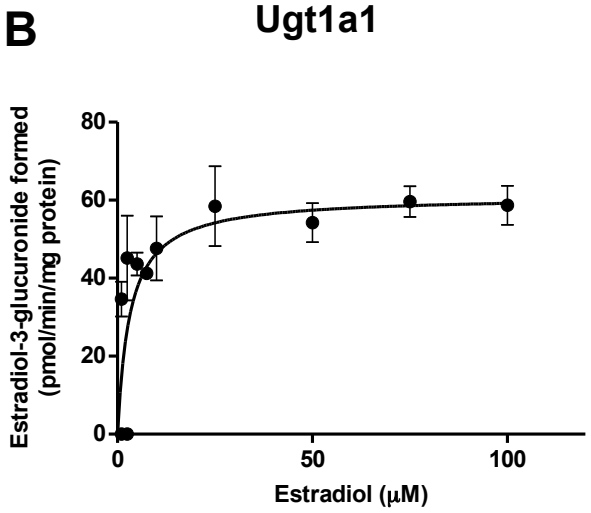

Kurita et al, Fig. 6